JOURNAL OF MATERIALS SCIENCE 33 (1998) 3031–3036

Microwave photodielectric and photoconductivity studies of commercial titanium dioxide pigments: the influence of transition metal dopants

R. JANES, M. EDGE, J. ROBINSON, N. S. ALLEN, F. THOMPSON
Department of Chemistry and Materials, Manchester Metropolitan University, John Dalton Building, Chester Street, Manchester M1 5GD, UK
E-mail: r.janes@mmu.ac.uk

The effect of transition metal ion doping on the charge carrier dynamics in commercial TiO_2 pigments has been investigated. The response to extended polychromatic irradiation was monitored by real-time measurements of microwave photoconductivity and photodielectric effects. In addition to intrinsic differences between the rutile and anatase polymorphs, shifts in the resonance frequency and quality factor of a tuned microwave cavity as a function of annealing, and foreign-ion incorporation provided a gauge of the influence of extrinsic trapping centres on photoactivity. Parallel luminescence studies revealed an extension in the lifetime of the emission band on doping, the energy associated with recombination being independent of the dopant ion. © *1998 Kluwer Academic Publishers*

1. Introduction

The commercial applications of metal oxide pigments are widespread. Titanium dioxide, in particular, possesses a high refractive index and low visible absorption, which makes it the most important white pigment in the paint, plastic and paper industries. Oxygen-deficient TiO_2 is an n-type semiconductor, in addition to being photoconductive on excitation by incident radiation of energy > 3.05 eV for the rutile polymorph and > 3.29 eV for the anatase form. The problematic photo-oxidation of polymeric binders by TiO_2, i.e. "chalking" in paints, is a consequence of free-radical formation at pigment surfaces, initiated by reaction of photoholes with surface hydroxyl ions [1]. This is followed by detrimental free-radical attack on the polymer host. Conversely, reactions such as these underpin photocatalytic applications of TiO_2, including the decomposition of organic pollutants [2, 3], reduction of carbon dioxide [4], or as a component of photoelectrochemical cells [5]. Clearly, inhibition of this process may be achieved by increasing the efficiency of electron–hole recombination in the bulk pigment, thus preventing surface reaction. Substitutional transition metal ion dopants would be expected to modify redox processes and the nature of the coupling between pigment particle and matrix. In this regard, Lou and Gao used surface photovoltage measurements to demonstrate a decrease in photoactivity and reduced chalking on doping with transition metals [6].

A consideration of the literature to date reveals any modification to the photoresponse of TiO_2 by transition-metal-ion substitution, to be dopant dependent. No attempt will be made here to present a comprehensive review, although the data for impurity ferric ions (one of the most widely studied dopants) will be briefly considered, to emphasize the salient features of this general approach and the methodology typically employed to evaluate the photoresponse. Moser *et al.* reported an extension of the lifetime of photocarriers from nanoseconds to minutes in aqueous colloidal TiO_2 on doping with Fe^{3+} [7]. Electron paramagnetic resonance (EPR) spectra were interpreted as a convolution of signals from Fe^{3+} centres substituted for lattice Ti^{4+} $(g = 1.99)$ and Fe^{3+} ions located next to charge-compensating anion vacancies $(g = 4.29)$. On bandgap exposure the spectra were characterized by the evolution of a signal assigned to Ti^{3+} centres, accompanied by the diminution of the low-field Fe^{3+} resonance. The overall response was attributed to hole trapping by Fe^{3+} and electron trapping by Ti^{4+}. It was also suggested that the locally uncompensated Fe^{3+} sites also act as electron traps, on the basis of changes in intensity of the $g = 1.99$ signal on exposure. Indeed, a subsequent study by Soria *et al.* revealed bulk Fe^{3+} ions to be more efficient electron traps than Ti^{4+} [8]. In a wider sense, parallel photocurrent and EPR measurements by Mizushima *et al.* identified the dopant energy levels of a range of polyvalent first-row d-block ions within the overall band picture of TiO_2 [9]. However, as discussed by Cox [10], it is important to exercise caution when considering such treatments.

In this work, we report some recent data on transition-metal-doped commercial TiO_2 pigments supplied by Tioxide Group UK. This forms part of a wider study of the application of microwave cavity perturbation techniques to determine pigment

0022–2461 © *1998 Kluwer Academic Publishers*

photoactivity in practical polymeric systems [11–14]. Microwave methodology, which has been extensively applied to semiconductors [15] and photographic materials [16], circumvents contact problems, and provides a simple and direct means of probing charge carrier dynamics in practical systems. The electronic processes in samples exposed to prolonged polychromatic radiation in a tuned microwave cavity were studied here; this is in contrast to the more extensively reported pulsed techniques [17–19]. However, we have recently demonstrated a clear correlation between time-resolved measurements and the real-time approach reported here [14]. Thus the aims of the present work were two-fold: to examine the effect of first-row d-block metal ion dopants on the photoactivity of practical TiO_2 pigments, and to evaluate the utility of real-time microwave cavity perturbation methods as a gauge of the charge carrier dynamics in such systems.

2. Experimental procedure

Titanium dioxide pigments were supplied by Tioxide Group Services Ltd, UK. Specifications for the parent materials (labelled according to their commercial designations for the sake of brevity) were as follows: HPT-3, 99.9% rutile, with crystallite size 0.1–0.5 μm, and SEL-AHR, uncoated anatase, crystallite size ~ 0.15 μm. Both materials were uncoated, and nominally of high purity. Doped samples were prepared by forming a slurry of the pigment in an aqueous solution of the metal salt. Following stirring, the samples were dried and fired in air at 800 °C to disperse the dopant into the lattice.

Microwave measurements were carried out using a Marconi 6310 programmable sweep generator (2–20 GHz) connected to a Marconi 6500 automatic amplitude analyser. A home-built cylindrical cavity was employed. Actinic radiation was provided by a Rank Aldis projector with tungsten light bulb, rated at 240 V, 250 W. It should be emphasized that the microwave data in our experimental configuration will represent a lower limit for photoactivity, given incomplete sample exposure. All samples were exposed to 1800 s polychromatic irradiation, followed by 1800 s dark decay, with continuous monitoring of the microwave response during these periods.

Luminescence measurements were carried out using a Perkin-Elmer LS50-B spectrometer operating at 77 K. Anatase samples were excited at 340 nm and emission monitored over 360–680 nm. For rutile samples, excitation was set at 370 nm, and the emission spectra recorded over 760–900 nm.

X-ray powder diffraction patterns were obtained using a Philips PW3020 diffractometer employing CuK_α radiation.

3. Results and discussion

Fig. 1 shows a plot of the shift in cavity resonance frequency during successive periods of exposure and darkness for the HPT-3 powders, both undoped and doped (only two examples of the latter are shown for clarity). Full details of the microwave apparatus and methodology employed, together with a discussion of the interpretation and significance of the data obtained, are detailed elsewhere [13, 14]. It should be noted that, in all cases, the cavity resonant frequency does not decay back to its initial value prior to irradiation. This implies the existence of long-lived trapped carriers, even following 30 min in darkness at room temperature. This result is not unexpected, given that Addis *et al.* [20] have demonstrated the persistence of luminescence emission bands up to 100 °C in rutile single crystals. Furthermore, application of Fermi level analysis to thermally stimulated current data, demonstrated the existence of electron traps of depths up to 0.87 eV [20].

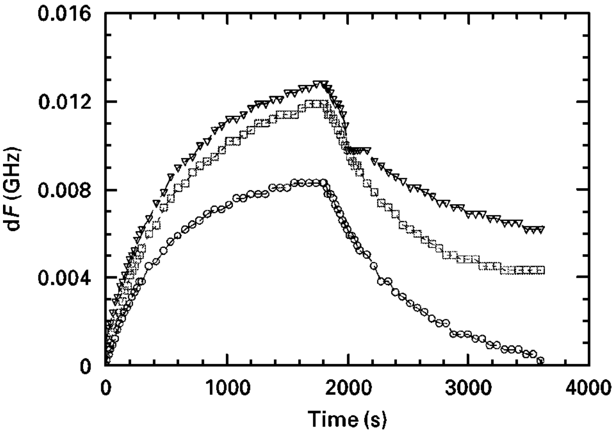

Figure 1 Changes in microwave resonant frequency for doped ((▽) copper and (□) iron) and (○) undoped rutile HPT-3 powders during 1800 s polychromatic exposure and 1800 s in darkness.

The complete frequency data for the rutile samples are given in Table I. In general, it is clear that all samples (with the exception of the manganese-doped material) show a reduction in the half-life of the frequency decay, $T_{1/2}$, on removal of the incident light source, suggesting that the dopants have introduced new states into the bandgap which enhance the efficiency of recombination. The magnitude of the frequency shift, dF, both during exposure and dark decay shows very little variation over the whole series. We suggest that the anomolous data for the manganese-substituted sample may arise from ineffective incorporation of this particular dopant into the host lattice under our preparative conditions and will not be considered further here.

Numerous attempts have been made to characterize the energy levels of traps within the bandgap of TiO_3. Given that the microwave measurements are probing carrier trapping, presumably fundamental to recombination channels, a correlation with more conventional luminescence data should be apparent. Following bandgap exposure, phosphoresence measurements reveal a green emission at 540 nm for the anatase polymorph assigned to a self-trapped exciton [21]. In rutile, near-bandgap emission is thought to originate from free Wannier-type excitons, with a weak near-infrared band being attributed to recombination at impurity Cr^{3+} centres [22–24]. From studies of commercial pigments by Allen *et al.* [25], the nature of the

TABLE I Frequency parameters for HPT-3 samples doped with first-row transition metal ions

Sample	F_{initial} (GHz)	dF_{max} after 30 min irradiation (GHz)	$T_{1/2}$ microwave F dark decay (s)	F_{final} after 30 min dark decay (GHz)
HPT-3	5.4145	0.012 60	816	5.4188
HPT-3 (fired)	5.4409	0.008 32	456	5.4411
HPT-3 (Cr-doped)	5.4182	0.009 29	536	5.4197
HPT-3 (Mn-doped)	5.4219	0.010 16	1010	5.4259
HPT-3 (Fe-doped)	5.4086	0.012 84	789	5.4148
HPT-3 (Co-doped)	5.4291	0.009 21	650	5.4312
HPT-3 (Ni-doped)	5.4143	0.009 77	628	5.4162
HPT-3 (Cu-doped)	5.4409	0.011 94	629	5.4452
HPT-3 (Zn-doped)	5.3987	0.009 71	650	5.4013

emission from rutile was found to be dependent on which of the two common commercial preparative routes were employed (i.e. the “sulphate” or “chloride” processes). Bands were detected at 830 nm from rutile synthesized by the “sulphate” route, or 1015 nm from a “chloride”-produced pigment [25].

TABLE II Phosphorescence lifetimes for doped HPT-3 samples

Sample	Phosphorescence lifetime (ms)
HPt-3 (undoped)	0.8226
HPT-3 (fired)	1.5731
Cr	1.5329
Mn	3.1327
Fe	3.1941
Co	1.7239
Ni	1.6428
Cu	2.1911
Zn	2.0547

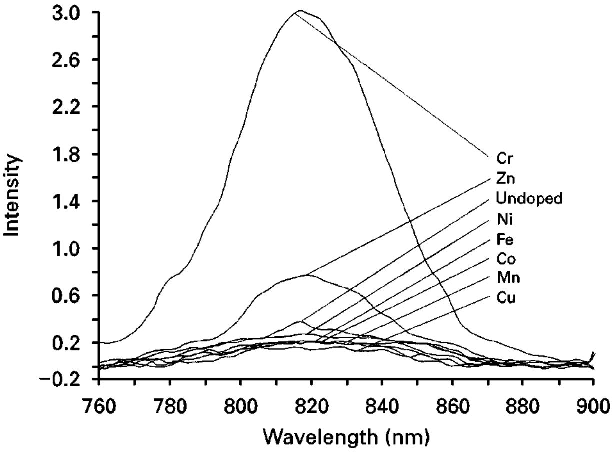

Figure 2 Luminescence spectra measured at 77 K for HPT-3 doped with various transition metals.

The emission from the HPT-3 pigments was monitored in the near-infrared region during continuous band-gap excitation at 77 K. Table II summarizes the data obtained. The increased lifetime in the doped samples and the annealed undoped material is indicative of a greater concentration of localized centres in the treated materials. Fig. 2 shows the photoluminescence spectra for the doped rutile samples, where, interestingly, the energy associated with the emission from all samples shows little variation, all lying in the range 0.95–0.97 eV. This implies the dominant recombination mechanism at 77 K, in these pigments, is essentially independent of the nature of the dopant. This somewhat intriguing result is in contrast to a system such as the well-studied II/VI semiconductor, ZnS, where doping with copper, silver and manganese produces different Stokes’ shifts [26]. Furthermore, the intensity of the emission from HPT-3 does vary markedly with dopant, the strongest band arising from the chromium-doped sample, with the intensity of the band from the zinc-doped material also clearly enhanced relative to the undoped state.

A parallel series of experiments was carried out using the commercial anatase pigment (SEL-AHR). Once again, a significant reduction in the half-life of the frequency decay was observed (Table III), although, interestingly, doping produced negligible changes in phosphorescence lifetimes, suggesting a relatively high concentration of traps in the parent materials compared with HPT-3. In general undoped SEL-AHR has a longer phosphorescence lifetime than HPT-3, which underlines our general observations for undoped anatase and rutile, respectively [13]. Photoluminescence spectra for doped anatase are shown in Fig. 3. Once again, emission occurred at the same wavelength over the whole series (~580 nm), with the highest intensity band being detected for the chromium-doped material.

X-ray powder diffraction revealed no evidence for the anatase-to-rutile phase transition as a result of the heat treatment carried out here, although we cannot rule out the presence of levels of rutile below the X-ray diffraction (XRD) detection limits arising from the early stages of the nucleation-and-growth process. The presence of rutile regions within an anatase matrix would be expected to modify the photoactivity of the pigment in addition to any dopant-induced modification. In the mixed-phase Degussa P25 (~75% anatase), Warman *et al.* [17] have suggested photoelectrons become localized in rutile regions, a consequence of the higher level of the conduction band in anatase and the assumption of a sintered cluster microstructure.

Furthermore, for samples of both rutile and anatase, we also note a significant enhancement in $T_{1/2}$ from the annealed undoped parent material. Clearly such a heat treatment would be expected to remove structural singularities which could act as recombination centres, and the observed lifetime

TABLE III Frequency parameters for SEL-AHR samples doped with first-row transition metal ions

Sample	F_{initial} (GHz)	dF_{max} after 30 min irradiation (GHz)	$T_{1/2}$ Microwave F dark decay (s)	F_{final} after 30 min dark decay (GHz)
Sel-AHR	5.4541	0.01210	806	5.4582
Sel-AHR (fired)	5.5076	0.00463	660	5.5087
Sel-AHR (Cr-doped)	5.4552	0.00649	569	5.4562
Sel-AHR (Mn-doped)	5.4672	0.00621	472	5.4679
Sel-AHR (Fe-doped)	5.4715	0.00659	693	5.4732
Sel-AHR (Co-doped)	5.4920	0.00730	585	5.4932
Sel-AHR (Ni-doped)	5.4528	0.00814	542	5.4538
Sel-AHR (Cu-doped)	5.4508	0.00785	628	5.4527
Sel-AHR (Zn-doped)	5.4580	0.00555	488	5.4578

increase is somewhat unexpected. However, we may speculate that impurities have been either inadvertantly introduced during heating, or a more homogeneous distribution of existing impurities has formed at elevated temperatures. In this regard, TiO_2 samples subjected to a range of physical and chemical treatments have been examined by Heller *et al.* [27]. These workers claim that, for reduced pigments, where bulk defect recombination dominates the photoprocesses, milling decreases photoactivity, whilst an enhancement is observed on removal of lattice defects by etching. Clearly, sample handling and mechanical treatments are important contributory factors defining pigment photoactivity.

The overall change in microwave power following exposure to incident light is indicative of the concentration of photoproduced free carriers. The shift in the cavity quality factor, Q, is a result of the interaction of free carriers with the electric field vector of the microwaves. For both polymorphs, the overall change in power for all doped and fired samples during irradiation is positive, indicating a reduction in the free carrier concentration relative to the host material [28, 29].

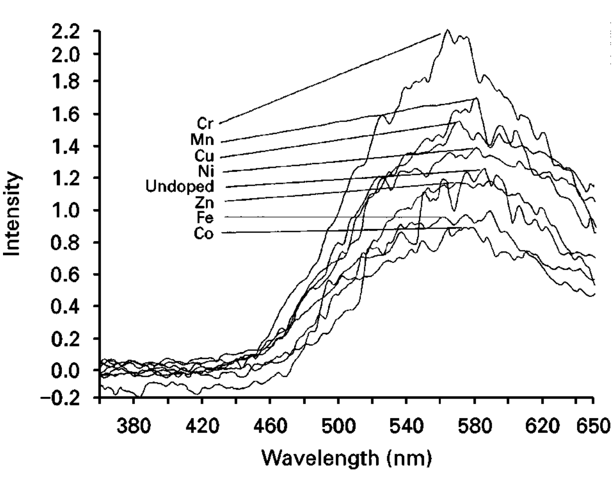

Figure 3 Luminescence spectra measured at 77 K for SEL-AHR doped with various transition metals.

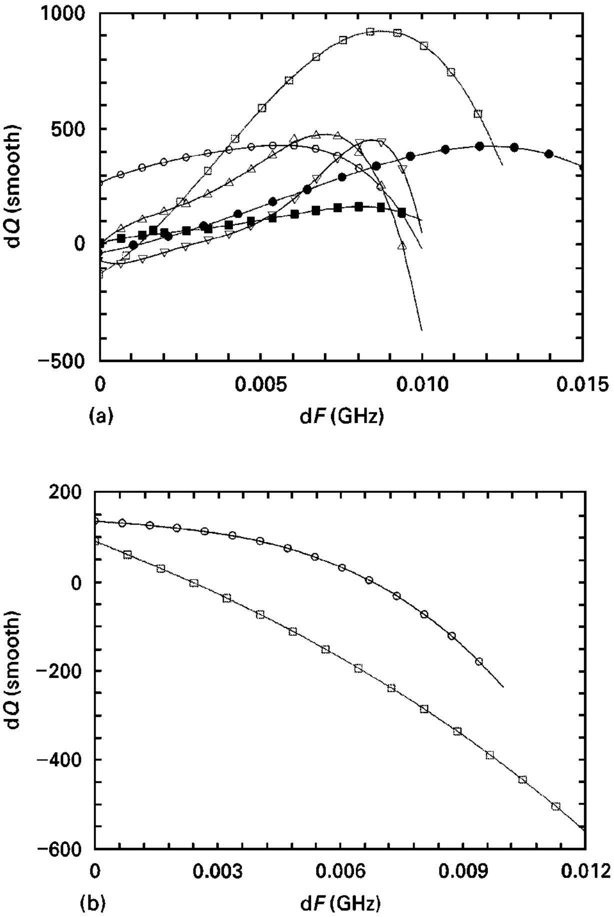

Figure 4 Change in microwave quality factor versus change in resonant frequency for HPT-3 rutile samples under 1800 s polychromatic radiation: (a) (△) undoped and doped with (■) nickel, (●) iron, (▽) cobalt, (□) copper and (○) zinc; (b) doped with (□) manganese and (○) chromium.

Fig. 4a and b shows a plot of dQ as a function of dF during polychromatic irradiation of rutile. Here there is a clear increase in free carriers as the sample becomes more polarizable (increasing dF) on irradiation. The nickel- and zinc-doped samples show a slower build up of conductivity than the more photoactive copper- and iron-doped materials. In contrast, the manganese- and chromium-doped materials showed a decrease in dQ as the sample becomes more polarizable. A series of corresponding measurements on anatase samples is presented in Fig. 5a–c. The undoped SEL-AHR exhibits an increase in dQ as the sample becomes more polarizable, which is also observed for the nickel- and cobalt-doped materials, albeit at a reduced level. Conversely, the other doped pigments show a decrease in dQ as a function of dF, which is contrary to the observations for the doped

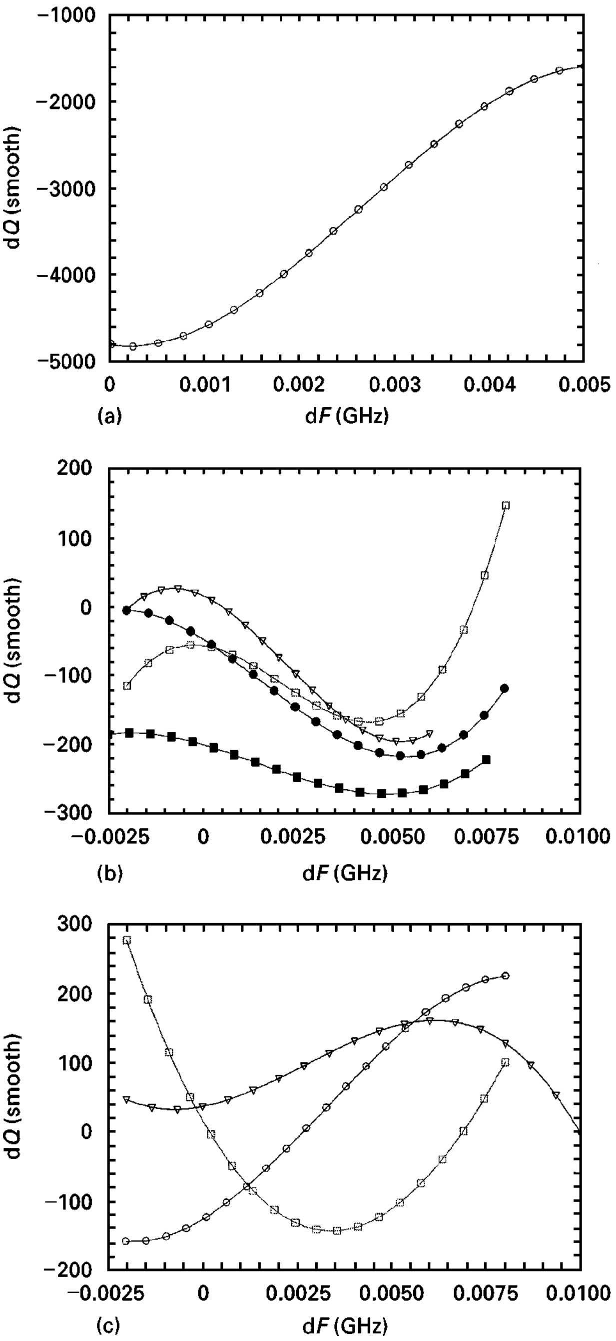

Figure 5 Change in microwave quality factor versus change in resonant frequency for SEL-AHR anatase samples under 1800 s polychromatic radiation: (a) undoped; (b) doped with (■) chromium, (●) iron, (▽) zinc and (□) manganese; (c) doped with (▽) nickel, (□) copper and (○) cobalt.

rutile pigments. An increase in dQ with dF indicated that more free carriers are produced than are being trapped out, although it should be noted that for low mobility semiconductors, such as TiO_2, microwave absorption may also contain an additional contribution from trapped carriers, which may, in this case, be small polarons or $Ti^{3+}(d^1)$ centres.

4. Conclusion

From the study it is apparent that incorporation of transition metal ions into pigmentary titanium dioxide markedly affects photoactivity during exposure to polychromatic radiation. Most notably, significant decreases in the frequency decay half-life was symptomatic of enhanced carrier recombination, and as such should lead to supression of photocatalytic behaviour. However, from a more fundamental viewpoint, the response is apparently highly complex. Presumably a range of factors such as oxidation state and chemical environment of the dopant, dopant distribution, homogeneity, particle size, morphology and microstructure, will dictate the behaviour. The preparative conditions employed here would nominally be expected to give rise to dopant ions in their highest oxidation states, although factors such as crystal-field stabilization in specific local coordination geometries would be expected to yield alternative states, thus determining the location of the d-electron manifolds within the bandgap.

The luminescence spectra for both crystalline forms showed the highest intensity emission from chromium-doped samples, which interestingly has long been identified as the recombination centre in nominally pure rutile, responsible for the broadband emission in the infrared region. However, given the observation that the wavelength of emission is essentially independent of dopant ion, the notion of simple impurity-induced recombination, is clearly called into question.

We conclude that, although the nature of the recombination centres is not apparent, the conjoint microwave and luminescence study reported here augments the available data in this somewhat controversial area. In this regard, further studies are currently underway to elucidate in greater depth the nature of the modifications to the photochemistry of titanium dioxide produced by transition metal ion doping. Certainly, the value of the microwave technique described here, as a gauge of the photoactivity of practical pigments, is clearly demonstrated.

Acknowledgement

The authors thank Tioxide UK for providing samples and for technical advice during the course of this work.

References

1. L. E. BROOKES, P. SENNET and H. H. MORRIS, *J. Paint Tech.* **39** (1967) 472.
2. A. M. LINESEBIGLER, G. YU and J. T. YATES, *Chem. Rev.* **95** (1995) 735.
3. D. F. OLLIS, E. PELIZZETTI and N. SERPONE, *Environ. Sci. Technol.* **25** (1991) 1523.
4. Z. GOREN, I. WILLNER, A. J. NELSON and A. J. FRANK, *J. Phys. Chem.* **94** (1990) 3784.
5. A. HAGFELDT and M. GRATZEL, *Chem. Rev.* **95** (1995) 49.
6. Z. LUO and Q. H. GAO, *J. Photochem. Photobiol. A Chem.* **63** (1992) 367.
7. J. MOSER, M. GRATZEL and R. GALLAY, *Helv. Chim. Acta* **70** (1987) 1596.
8. J. SORIA, J. C. CONESA, V. AUGUGLIARIO, L. PALMISANO, M. SCHIAVELLO and A. ACLAFANI, *J. Phys. Chem.* **95** (1991) 274.
9. K. MIZUSHIMA, M. TANAKA, A. ASAI, S. IIDA and J. B. GOODENOUGH, *J. Phys. Chem. Solids* **40** (1979) 1129.
10. P. A. COX, "Transition Metal Oxides", (Oxford University Press, Oxford, 1992) p. 128.

11. N. S. ALLEN, M. EDGE, J. H. HE and F. THOMPSON, *Dyes Pigments* **20** (1992) 211.
12. M. EDGE, J. ROBINSON, N. S. ALLEN and R. JANES, *Polym. Preprints* **34** (1993) 220.
13. J. ROBINSON, PhD thesis, Manchester Metropolitan University (1996).
14. M. EDGE, R. JANES, J. ROBINSON, N. S. ALLEN and J. M. WARMAN, *J. Photochem. Photobiol*, accepted for publication.
15. J. M. WARMAN, M. P. de HASS, M. GRATZEL and P. P. INFELTA, *Nature* **310** (1984) 305.
16. J. P. SPOONHOWER, *Photogr. Sci. Eng.* **24** (1980) 130.
17. J. M. WARMAN, M. P. de HASS, P. PICHAT, T. P. M. COSTER, E. A. VAN der ZOUWEN-ASSINK, A. MACKOR and R. COOPER, *Radiat. Phys. Chem.* **37** (1991) 433.
18. S. T. MARTIN, H. HERRMAN, W. CHOI and M. R. HOFFMANN, *J. Chem. Soc. Farad. Trans.* **90** (1994) 3315.
19. *Idem., ibid.* **90** (1994) 3323.
20. R. R. ADDIS, A. K. GHOSH and F. C. WATKIM, *Appl. Phys. Lett.* **12** (1968) 297.
21. H. TANG, H. BERGER, P. E. SCHMID and F. LEVY, *Solid State Commun.* **87** (1993) 847.
22. L. G. J. de HAART and G. BLASSE, *J. Solid. State Chem.* **61** (1986) 135.
23. A. K. GHOSH, R. B. LAUER and R. R. ADDISS, *Phys. Rev.* **8** (1973) 4842.
24. A. AMOUT and R. LEONELLI, *Solid State Commun.* **84** (1992) 349.
25. N. S. ALLEN, D. J. BULLEN and J. F. McKELLAR, *Chem. Ind.* (1978) 630.
26. R. H. BUBE, "Photoelectronic Properties of Semiconductors", (Cambridge University Press, Cambridge, 1992) p. 142.
27. A. HELLER, Y. DEGANI, D. W. JOHNSON Jr and P. K. GALLAGHER, *J. Phys. Chem.* **91** (1987) 5987.
28. W. H. HARTWIG and J. J. HINDS, *J. Appl. Phys.* **40** (1969) 2020.
29. Y. WATANABE, *ibid.* **57** (1985) 2613.

Received 20 August 1997
and accepted 24 March 1998